Outgoing boundary conditions for finite-difference elliptic water-wave models

By Bingyi Xu and Vijay Panchang

Civil Engineering Department, University of Maine, Orono, Maine 04469, U.S.A.

Two-dimensional elliptic water-wave models based on the mild-slope equation find wide application in engineering and other studies. Model results are often adversely influenced by approximate treatment of the open boundary condition. A method to incorporate the exact radiation condition at infinity in finite-difference models is therefore developed. Since directly matching the solutions within the computational domain to those outside is too stringent a requirement, the new method is based on minimizing the overall discrepancy between the solutions along the open boundary. This relaxation permits the development of a suitable solution method, which is tested against analytical solutions for two situations. Satisfactory results are obtained with no artificial reflection of wave energy from the open boundary, even when it is placed very close to the scatterer.

1. Introduction

The 'mild-slope' equation, also known as the combined refraction–diffraction equation (Berkhoff 1976), has received wide acceptance for performing engineering simulations of wave propagation over arbitrary bathymetry and in complex coastal domains. It can model the propagation of a wide spectrum of waves, from short waves to long waves, and it has been successfully used (sometimes with appropriate modifications) to simulate wave propagation in harbours, around breakwaters and floating structures, in open coastal areas, in regions with marine vegetation, around islands, etc. (See Panchang *et al.* (1991) for a list of references.)

While developing a computational model for the mild-slope wave equation, one often encounters considerable difficulty in the treatment of the 'open' boundary (where the computational domain intersects the surrounding sea). This boundary contains (possibly in addition to a specified incident wave) 'scattered' waves that arise from bathymetric effects and/or the presence of other (possibly reflecting) boundaries. The scattered waves are not known *a priori*, and indeed the goal of the modelling is the quantification of precisely these waves. Usually, therefore, the open boundary is placed far enough away from the area of interest in the model, in the hope that imprecise boundary conditions will not affect the results in this area. This of course results in increased computation.

The mild-slope wave model is sometimes solved via the 'parabolic approximation'. In this method, a dominant wave direction is chosen (say x; $x \geqslant 0$) and wave spreading in only a limited aperture (typically about $\pm 45°$) about the $+x$-axis is allowed. Wave propagation in the $-x$ direction is also assumed to be negligible. The upwave boundary ($x = 0$) of the computational domain ($x \geqslant 0$; $a \leqslant y \leqslant b$) contains only specified incident waves. Difficulty with the treatment of open boundaries can thus arise only on the two lateral boundaries ($y = a$ and $y = b$). Recently, however,

Proc. R. Soc. Lond. A (1993) **441**, 575–588
Printed in Great Britain

Dalrymple & Martin (1992) have devised an eminently satisfactory method of treating such boundaries in parabolic models, using an assumption of constant depths outside these boundaries. The lateral boundary conditions are derived in terms of an integration of quantities along the boundary. This allows waves to exit the computational region with no spurious reflections from the open boundary.

In the context of the full elliptic mild-slope wave models, boundary conditions may have to be specified for several open boundaries with arbitrary configurations (depending on the complex shape of the harbour, etc.). Approximate outgoing boundary conditions were utilized in elliptic models by Berkhoff *et al.* (1982) and Panchang *et al.* (1988, 1991), on the assumption that all outgoing waves exited the domain in a direction perpendicular to the boundary. This assumption is clearly not true for all wave components and, as noted by Kirby (1989), can lead to spurious oscillations in the solution. To alleviate this limitation of normal incidence along the outgoing boundary, Kirby (1989) has proposed the use of various parabolic approximations as boundary conditions for the scattered waves; these parabolic equations can accommodate waves exiting through a larger aperture (noted earlier). However the aperture is still limited. In addition, the very nature of the parabolic equation requires, *a priori*, the selection of the 'dominant' direction for the exiting waves (which may not be known) and the placement of the open boundary in a direction perpendicular to it. This can be problematic in domains of complex shape, particularly if several incident wave directions are to be treated.

Rather than approximate the actual boundary conditions, the modeller may prefer to approximate the bathymetry and represent the sea region outside the computational domain by a constant depth. (This is probably a good approximation for short waves outside the open boundary since it may be deep water.) With this assumption, it is possible to exactly describe the properties of the scattered waves outside the computational domain (although an exact boundary condition itself is not explicitly obtained.) The scattered waves must satisfy the radiation condition at infinity, and they can be described by a Bessel–Fourier series. Within the finite-element framework, this information can be utilized through the use of a 'superelement'. The radiation condition at infinity is naturally incorporated into the variational formulation, and no spurious reflections arise. (See Mei (1983) for details.) Finite-element models of this type have been developed by Houston (1981), Tsay & Liu (1983), Kostense *et al.* (1986), and Chen & Houston (1987).

Despite the success of finite-element models in treating the open boundaries, they can be cumbersome to construct and apply. For instance, finite-element grid-generation and modification may be a major task even at present. (Grid-generation for the Kawaihae harbour (Hawaii) took several weeks at the US Army Waterways Experiment Station (Lillycrop *et al.* 1990)). Finite-difference elliptic models are therefore sometimes preferred, due to their simplicity and ease of construction and implementation. Finite-difference models for very large wave problems have been recently developed by Panchang *et al.* (1988, 1991) and by Li & Anastasiou (1992). They all suffer from inadequate treatment of the open boundary conditions, though, and this problem has stood in the way of further development of such models. The object of this paper, therefore, is to incorporate the exact radiation condition at infinity in a finite-difference model. Unlike finite-element models, this condition does not enter naturally into the scheme. However, we use an optimization criterion to relate the solutions inside and outside the computational domain. As in the case of the 'perfect' treatment of open boundary conditions for parabolic models (Dalrymple

& Martin 1992) and also the approximate formulations of Kirby (1989) for elliptic models, all points on the open boundary now get connected, and an appropriate numerical solution methodology is devised.

The layout of the paper is as follows. Section 2 gives a mathematical description of the problem from a modelling viewpoint. In §3, a solution procedure is derived. Section 4 deals with implementation of the procedure and a solution algorithm is developed. In §5, the scheme is tested for two cases for which analytical solutions are available. Section 6 summarizes the study and offers concluding remarks.

2. Problem statement

The combined refraction-diffraction equation (Berkhoff 1976; Smith & Sprinks 1975) that describes the propagation of periodic, small-amplitude, surface gravity waves over an arbitrarily varying, mild-sloped sea-bed is:

$$\nabla\cdot(CC_{\mathrm{g}}\nabla\phi)+(C_{\mathrm{g}}/C)\,\sigma^2\phi=0, \tag{1}$$

where $\phi(x,y)$ is the complex surface elevation function, from which the wave height can be estimated; σ is the wave frequency under consideration; $C(x,y)$ is the phase velocity (σ/κ); $C_{\mathrm{g}}(x,y)$ is the group velocity $(\partial\sigma/\partial\kappa)$; $\kappa(x,y)$ is the wavenumber $(=2\pi/L)$, related to the local depth $d(x,y)$ through the dispersion relation:

$$\sigma^2=g\kappa\tanh(\kappa d). \tag{2}$$

Instead of working with (1), it is convenient to work with the following wave equation:

$$\nabla^2\Phi+K^2(x,y)\,\Phi=0 \tag{3}$$

which is obtained from (1) through the transformation suggested by Radder (1979):

$$\Phi=\phi(CC_{\mathrm{g}})^{0.5}\quad\text{and}\quad K^2=\kappa^2-\nabla^2(CC_{\mathrm{g}})^{0.5}/(CC_{\mathrm{g}})^{0.5}. \tag{4}$$

In this formulation, Φ is a modified wave potential function and K is a modified wavenumber. Also, a rectangular domain is chosen for demonstration. The method can be easily applied to non-rectangular regions, with internal boundaries when necessary, as shown later. The domain, coordinate axes, incident wave direction, etc., are shown in figure 1.

The domain is discretized into finite-difference grids of size Δx and Δy. If Φ_j^i is used to denote the grid-point value of the potential, standard discretization of (3) using second-order finite-differences (for $\Delta x=\Delta y$) yields:

$$\Phi_j^{i-1}+\Phi_j^{i+1}+\Phi_{j-1}^i+\Phi_{j+1}^i+[(K\,\Delta x)^2-4]\,\Phi_j^i=0. \tag{5}$$

The conventional approach consists of writing such equations for all internal points in the domain. Inclusion of boundary conditions gives additional equations, and the resulting system of equations may be expressed in matrix form as:

$$[G]\{\Phi\}=\{f\}, \tag{6}$$

where $[G]$ is the system matrix, $\{\Phi\}$ is the unknown vector (of the desired grid-point values of the wave potential), and $\{f\}$ is a vector that contains information from the discretized boundary conditions, which have to be imposed along AC, BD, CD, and AB. When the boundaries represent seawalls, coastlines, etc., the following condition may be used (Berkhoff 1976; Kostense *et al.* 1986):

$$\partial\Phi/\partial n-\mathrm{i}K\alpha\Phi=0, \tag{7}$$

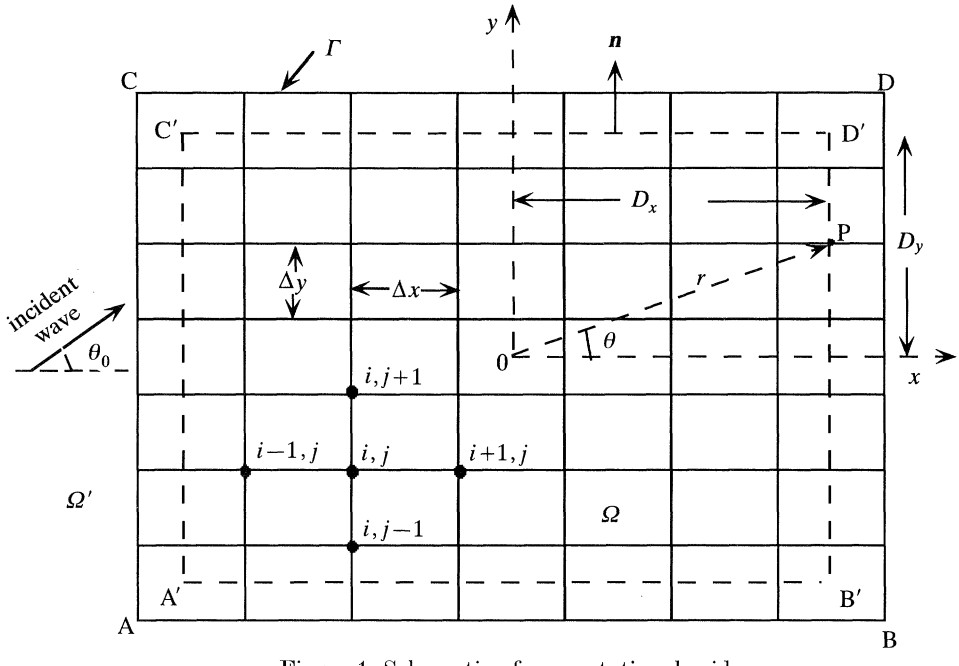

Figure 1. Schematic of computational grid.

where n is the direction normal to the boundary and α is a reflection coefficient that may have to be determined empirically. Incorporation of (7) into (6) is not difficult. However, along open boundaries, a suitable boundary condition is not available. Our goal is to devise a scheme for incorporating such boundaries in (6), and for demonstration, we assume that all four boundaries in figure 1 are 'open' boundaries. (Problems with other boundaries are also treated later.)

We assume that the sea outside the computational domain (denoted by Ω') is of constant depth. Varying bathymetry, internal boundaries (such as structures, islands, etc.) that cause scattering are assumed to be inside the computational region (denoted by Ω). In Ω', therefore, equation (1) reduces to the Helmholtz equation

$$\nabla^2\overline{\Phi}+K_c^2\overline{\Phi}=0, \tag{8}$$

where K_c represents the wavenumber over the constant depth. The solution of (8) is composed of two parts, the incident wave potential Φ^I and the scattered wave potential Φ^S, i.e.

$$\overline{\Phi}=\Phi^I+\Phi^S, \tag{9}$$

where

$$\Phi^I=A_0\exp[\mathrm{i}K_c r\cos(\theta-\theta_0)]. \tag{10}$$

In (10), A_0 and θ_0 are the amplitude and direction of the incident wave. Φ^S is the scattered wave potential that must satisfy (in addition to (8)) the radiation condition at infinity:

$$\sqrt{(K_c r)}\left(\frac{\partial}{\partial r}-\mathrm{i}K_c\right)\Phi^S\to 0, \quad K_c r\gg 1. \tag{11}$$

The required Φ^S is given by the following Fourier–Bessel series (Mei 1983):

$$\Phi^S=\alpha_0 H_0(K_c r)+\sum_{l=1}^{\infty} H_l(K_c r)\,(\alpha_l\cos l\theta+\beta_l\sin l\theta), \tag{12}$$

where $H_l(K_c r)$ is the Hankel function of the first kind and order l. The coefficients α_l and β_l are, however, not known. Equation (12) does provide information regarding the nature of the solution on the open boundary, though, and our objective is to incorporate this information in the finite-difference model for Ω.

3. Solution methodology

Continuity of the solution along the open boundary requires:

$$\Phi = \overline{\Phi}; \quad \Phi_n = \overline{\Phi}_n \quad \text{on } \Gamma, \tag{13a, b}$$

where the subscript n denotes the normal derivative. Theoretically, using discretized values for the terms on the left and analytical expressions for the terms on the right should give additional equations (containing the unknown coefficients α_l and β_l). These can be combined with the internal equations (5) and the resulting matrix can be solved. In practice, however, in the numerical model (for Ω), the boundary condition is satisfied only for the grid-point on Γ. The number of additional equations that these boundary points provide may be more or less than the actual number of equations required, which depends on the number of terms that are retained in the series (12). (For computational purposes, the series (12) has to be truncated after m terms, depending on the convergence. Usually m has to be found by trial-and-error.) The number m is typically far less than the number of boundary grid-points leading to an over-determined system of equations. Increasing the terms in series (12) to obtain an exact match between the number of equations and the unknown coefficients is cumbersome; not only is an inordinately large number of terms required, but the large magnitude of the high-order Hankel functions leads to an ill-conditioned coefficient matrix.

This difficulty with meeting the matching criteria (13) directly can be eliminated if we seek to obtain the coefficients α_l and β_l such that the following overall error functional is minimized:

$$F = \sum_{j=1}^{N} \left(\overline{\Phi}_j - \Phi_j \right)^2, \tag{14}$$

where j is a grid-point on Γ and N is the total number of points on it. Assuming that the series (12) has been truncated after m terms, define vectors:

$$\{h\}^{\mathrm{T}} = \{H_0, H_1 \cos\theta, H_2 \cos 2\theta, \ldots, H_m \cos m\theta; H_1 \sin\theta, H_2 \sin 2\theta, \ldots, H_m \sin m\theta\}, \tag{15}$$

$$\{\mu\}^{\mathrm{T}} = \{\alpha_0, \alpha_1, \alpha_2, \ldots, \alpha_m; \beta_1, \beta_2, \ldots, \beta_m\}. \tag{16}$$

These vectors, each containing $L = 2m+1$ elements, represent the known and unknown parts of (12). For convenience, the argument $(K_c r)$ of the Hankel functions has been dropped in (15). Note that $\{h\}^{\mathrm{T}}$ is a function of the boundary grid location j.

We can now write (9) as

$$\overline{\Phi} = \Phi^{\mathrm{I}} + \Phi^{\mathrm{S}} = \Phi^{\mathrm{I}} + \{h\}^{\mathrm{T}} \{\mu\}. \tag{17}$$

Minimizing F with respect to the constants to be determined,

$$\partial F / \partial \mu_i = 0, \quad i = 1, 2, \ldots, L, \tag{18}$$

where μ_i represents the ith term in (16). Using (14) and (17) and performing the differentiation for each μ_i leads to:

$$\sum_{j=1}^{N} (\overline{\Phi}_j - \Phi_j)(h_1)_j = 0, \quad \sum_{j=1}^{N} (\overline{\Phi}_j - \Phi_j)(h_2)_j = 0, \ldots,$$

$$\times \sum_{j=1}^{N} (\overline{\Phi}_j - \Phi_j)(h_i)_j = 0, \quad \sum_{j=1}^{N} (\overline{\Phi}_j - \Phi_j)(h_L)_j = 0, \quad (19)$$

where $(h_i)_j$ represents the ith term in (15) for the jth boundary point. Equations (19) can be written concisely if we define the following matrices:

$$[C] = [c_{ij}] = [(h_i)_j], \quad \text{dimension } L \times N, \quad (20)$$

$$[A] = [C][C]^{\mathrm{T}} \quad \text{dimension } L \times L \quad (21)$$

and vectors

$$\{\Phi^{\mathrm{I}}\}_{\Gamma} = \{\Phi^{\mathrm{I}}_1, \Phi^{\mathrm{I}}_2, \ldots, \Phi^{\mathrm{I}}_N\}, \quad (22)$$

$$\{\Phi\}_{\Gamma} = \{\Phi_1, \Phi_2, \ldots, \Phi_N\}, \quad (23)$$

where Φ^{I}_i represents the value of the incident wave at the ith grid-point on the boundary, and Φ_i represents the desired numerical solution at this location. Using (20)–(23) and (17), (19) becomes

$$[A]\{\mu\} = [C]\{\Phi\}_{\Gamma} - [C]\{\Phi^{\mathrm{I}}\}_{\Gamma}. \quad (24)$$

Solving (24) for $\{\mu\}$, we have

$$\{\mu\} = [R](\{\Phi\}_{\Gamma} - \{\Phi^{\mathrm{I}}\}_{\Gamma}), \quad (25)$$

where $[R] = [A]^{-1}[C]$ is determined ahead of time. Note that $\{\mu\}$ cannot be directly determined at this stage since $\{\Phi\}$ is not known. However, (13b) can now be used to provide an additional criterion. Since $\{\mu\}$ is a constant, (17) can easily be differentiated; and using (25), the criterion (13b) gives:

$$\Phi_n = \overline{\Phi}_n \equiv \Phi^{\mathrm{I}}_n + \{h_n\}[R](\{\Phi\}_{\Gamma} - \{\Phi^{\mathrm{I}}\}_{\Gamma}), \quad (26)$$

where

$$\{h_n\} = \left\{\frac{\partial H_0}{\partial n}, \frac{\partial H_1 \cos\theta}{\partial n}, \ldots, \frac{\partial H_m \cos m\theta}{\partial n}; \frac{\partial H_1 \sin\theta}{\partial n}, \ldots, \frac{\partial H_m \sin m\theta}{\partial n}\right\}. \quad (27)$$

Equation (26) is the desired Robbins-type condition on the open boundary for the computational domain Ω of a finite-difference model.

4. Implementation

The boundary condition (26) must now be adapted for use in a linear equation system solver. To illustrate, we apply it to the open boundary shown by the dashed line in figure 2, where the alphabet denotes a grid location. At point P, for example, $(\Phi^{\mathrm{I}}_n)_p$ is determined on the basis of the given incident wave condition (analytically). Similarly $\{h_n\}_p$ can also be computed at the outset. At P, discretizing (26) yields:

$$(\Phi_b - \Phi_a)/\Delta s = (\Phi^{\mathrm{I}}_n)_p + \{h_n\}_p[R](\{\Phi\}_{\Gamma} - \{\Phi^{\mathrm{I}}\}_{\Gamma}). \quad (28)$$

Similar application to other boundary points (like P′, etc.) results in a system of N equations which may be written in matrix form as:

$$[S][\{\Phi\}_{\Gamma} - \{\Phi\}_{\mathrm{int}}] = \{\Phi^{\mathrm{I}}_n\} + [h_n]_p[R](\{\Phi\}_{\Gamma} - \{\Phi^{\mathrm{I}}\}_{\Gamma}), \quad (29)$$

where $[h_n]$ is the $N \times L$ matrix obtained by combining vectors such as (27) for each boundary point, $\{\Phi\}_{\mathrm{int}}$ is the vector of internal points adjacent to Γ (such as Φ_a), and

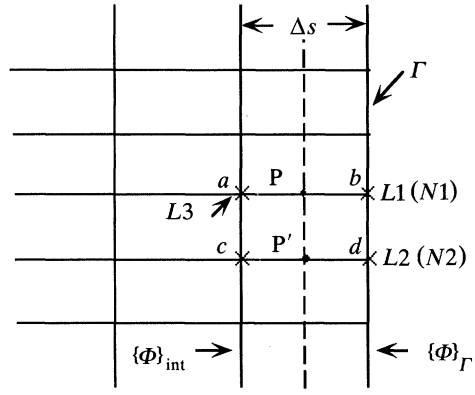

Figure 2. Definition sketch illustrating the location where boundary derivatives are computed and for transferring boundary information into global equation.

S is a diagonal matrix containing terms such as $1/\Delta x$, etc. The N linear equations (29) can be combined with the internal equations (5) (and the equations for other types of boundaries, e.g. those satisfying (7)), to obtain the final matrix equation (6).

The complete solution algorithm may be described as follows:

1. For each of the N grid points on the open boundary with grid coordinates (I, J), define a serial two-dimensional array $ID\ (K, 2)$, where $1 \leqslant K \leqslant \mathrm{N}$, such that $ID\ (K, 1) = I$ and $ID\ (K, 2) = J$ for the Kth boundary point.

2. For each K,

(a) knowing I and J (or x and y) find corresponding r, θ,

(b) use (15) to determine the Kth column of $[C]$ (equation 20),

(c) determine Kth element of the incident wave vector $\{\Phi^{\mathrm{I}}\}_{\Gamma}$ using (10).

This results in the matrix $[C]$ and vector $\{\Phi^{\mathrm{I}}\}_{\Gamma}$.

3. Find $[A] = [C][C]^{\mathrm{T}}$, $[A]^{-1}$ and $[R] = [A]^{-1}[C]$. Note that $[A]$ is typically a small matrix, its size being determined by the number of terms m retained in the series (12). Inverting A presents no difficulty.

4. For each K, find derivatives $[h_n]$ and $\{\Phi^{\mathrm{I}}_n\}$, as follows:

(a) The derivatives are computed at points such as P.

(b) Find the Kth row of $[h_n]$ by taking derivatives at P of the elements in vector $\{h\}$ defined in (15). This involves simple analytical differentiation. (See appendix.)

(c) Find the Kth element of $\{\Phi^{\mathrm{I}}_n\}$ by analytical differentiation of (10). (See appendix.)

5. Rewrite (29) as:

$$([B]-[S])\{\Phi\}_{\Gamma}+[S]\{\Phi\}_{\mathrm{int}} = -\{\Phi^{\mathrm{I}}_n\}+[B]\{\Phi^{\mathrm{I}}\}_{\Gamma}, \tag{30}$$

where $[B] = [h_n][R]$. Compute $[B]$ and the right-hand side vector $\{Q\} = -\{\Phi^{\mathrm{I}}_n\}+[B]\{\Phi^{\mathrm{I}}\}_{\Gamma}$, which will eventually go into $\{f\}$ of (6).

6. We now have to construct the final matrix equation (6). Let there be a total of LT' computational points (including all internal, open boundary, and other boundary points). Let the coordinates of the Lth grid point be (I, J).

(a) For all internal points, coefficients from (5) give the appropriate elements of $[G]$. Similarly at closed boundaries, elements of $[G]$ can be obtained by discretizing (7). It now remains to transfer the elements of the open boundary matrices (equation (30)) into the appropriate locations in $[G]$ and $\{f\}$. This is done as follows: Pick an element $B(N1, N2)$. Corresponding to $N1$, find $I1 = ID\ (N1, 1)$ and $J1 = ID\ (N1, 2)$. For

$I1$ and $J1$, find the corresponding grid point number $L1$ ($1 \leqslant L1 \leqslant LT$). Similarly for $N2$, find $L2$. The element $G(L1, L2)$ is then equal to $B(N1, N2)$. If $N1 = N2$, however, $G(L1, L2) = B(N1, N2) - 1/\Delta s$ (where $1/\Delta s$ arises from matrix $[S]$ and $\Delta s = \Delta x$ or Δy). The second term in (30) involves internal points adjacent to the boundary. Let $L3$ denote the location number of the appropriate internal point adjacent to $L1$. Then $G(L1, L3) = 1/\Delta s$.

(*b*) The elements of $\{Q\}$ also have to be transferred to $\{f\}$. The $N1$th element of $\{Q\}$ is equal to the $L1$th element of $\{f\}$.

7. Equation (6) can be solved by gaussian elimination or iterative schemes (Panchang *et al.* 1991; Li & Anastasiou 1992).

5. Verification

To examine the ability of the method described above to correctly handle open boundaries, two tests are performed. The first is the well-known problem of long waves propagating around a circular island located on a paraboloidal shoal (Homma 1950; Jonsson *et al.* 1976). The second is an investigation of harbour resonance.

(*a*) *Waves around an island*

The bathymetry for this case is shown in figure 3. This problem has been solved by Tsay & Liu (1987) and Houston (1981) by the finite-element method, using approximately 2304 and 5280 elements respectively. The finite-elements lie in a circular region covering the shoal.

We use a finite-difference grid (figure 4) containing only 31×31 grid points. The boundary condition along the island is given by (7) with $\alpha = 0$. These boundary derivatives, which are computed numerically, require the artificial inclusion in the computational module of some points which are really on the island. Hence, with the coarse resolution used here the circular island is not as well represented as in the finite-element model. The coarse resolution also affects the computation of K (equation (4)) for long waves at grid points along the island boundary; a depth equal to h_a was assumed to exist at just inside the island to facilitate the computation of the $\nabla^2(CC_g)^{0.5}$ term in (4). Similarly, the resolution also affects the estimation of K^2, which is discontinuous along the outer shoal boundary and influences the numerical results.

The 946 linear equations resulting from the procedure described in §4 were solved by gaussian elimination. Three sets of model results are shown in Figure 5 for wave periods $T = 240$ s, 410 s, and 480 s in the form of contour plots of the normalized wave height. Analytical solutions for this problem derived by Homma (1950), are also computed and shown. (The island appears as an octagon due to the finite-difference representation; see figure 4.) The model results compare extremely well with the analytical solutions. While there are some minor differences, the overall patterns exhibit no spurious reflection from the open boundaries. The differences may be attributed to the coarse grid and inexact representations for the island boundary and for the modified wave number.

(*b*) *Wave propagation in a rectangular harbour*

The second test of the solution method described in §4 involves the harbour resonance problem. This has become a standard test-case for many wave models (Chen & Houston 1987; Madsen & Larsen 1987; Panchang *et al.* 1991), and also exemplifies the difficulty with open boundaries in finite-difference models. The

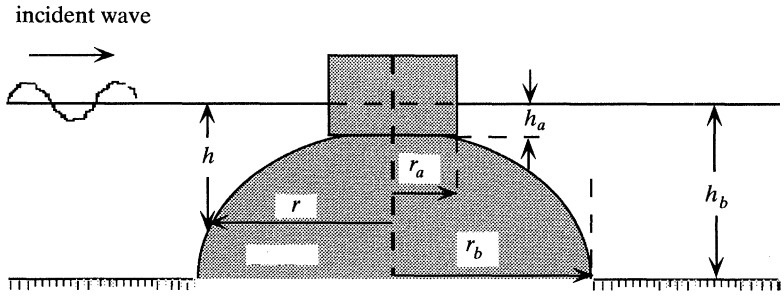

Figure 3. Circular island/shoal bathymetry; $r_a = 10^5$ m, $r_b = 3 \times 10^5$ m, $h_a = 0.444$ km, $h_b = 4$ km, $h = \alpha r^2$.

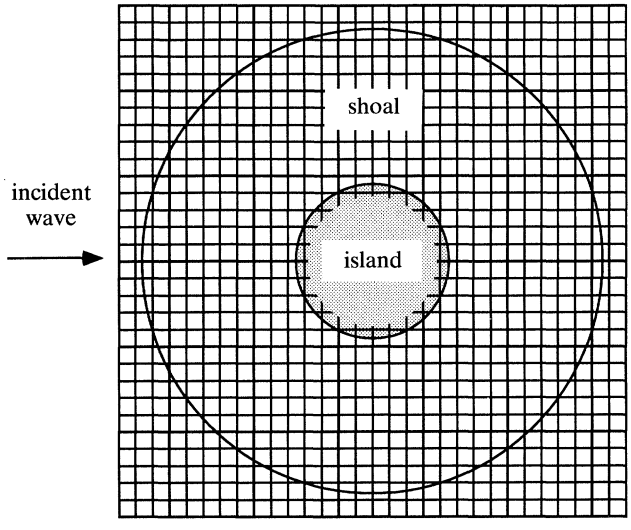

Figure 4. Finite-difference grid for wave propagation on island/shoal bathymetry.

domain consists of a rectangular harbour of constant depth surrounded by the open ocean (figure 6). To simulate the open sea with finite-difference models, Madsen & Larsen (1987) and Panchang *et al.* (1991) have included large rectangular regions (150 m × 30 m) outside the harbour within the computational domain, which contained over 4500 grids. Madsen & Larsen (1987) found that decreasing the size of the outer basin degraded their results. Using a different open boundary condition, Panchang *et al.* (1991) had to rely on artificial reflection coefficients to tune their model.

Here a finite-difference grid is constructed with a much smaller outer basin, 12 m wide and approximately 7 m long. However, for harbour problems, a slight modification to the procedure described in §4 is required, since the coastline outside the computational domain can create a reflected wave. The solution for the constant depth region can thus be treated as a combination of incident waves, reflected waves, and scattered waves, i.e. in Ω'

$$\overline{\Phi} = \Phi^{\mathrm{I}} + \Phi^{\mathrm{R}} + \Phi^{\mathrm{S}} = \Phi^{\mathrm{IR}} + \Phi^{\mathrm{S}}. \tag{31}$$

Φ^{IR}, the sum of the incident and reflected waves, is given by:

$$\Phi^{\mathrm{IR}} = A_0 \exp\left[\mathrm{i}K_{\mathrm{c}} r \cos(\theta - \theta_0)\right] + A_0 \exp\left[\mathrm{i}K_{\mathrm{c}} r \cos(\theta + \theta_0)\right], \tag{32}$$

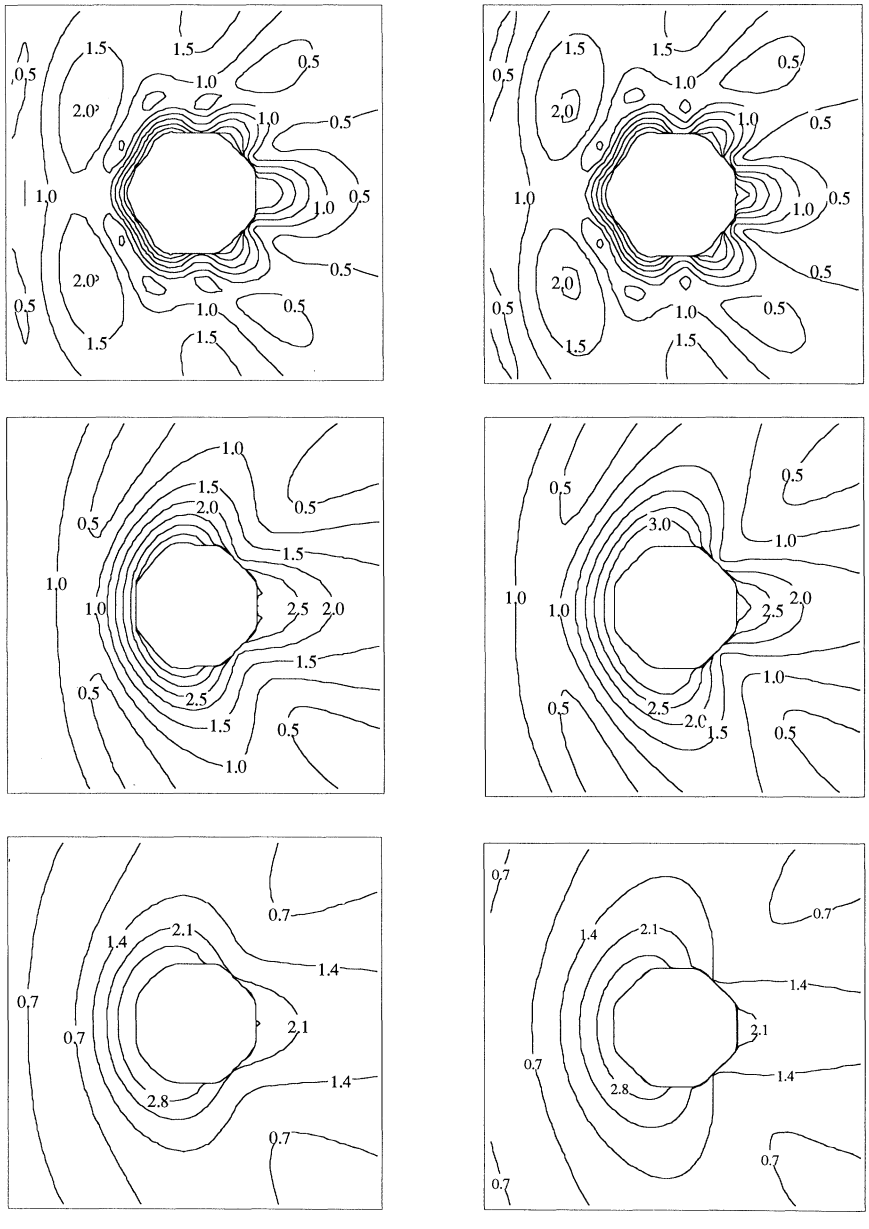

Figure 5. Wave height comparisons; finite-difference (left) and analytical (right). Period = 240 s (top); 410 s (middle); 480 s (bottom).

where, for simplicity, the coastline outside the computational domain has been assumed to be straight along the x-axis and fully reflecting. Requiring that

$$\partial \overline{\Phi}/\partial n = 0 \quad \text{along} \quad \theta = 0, \pi, \tag{33}$$

the scattered wave potential (equation (12)) now reduces simply to

$$\Phi^S = \sum_{l=0}^{\infty} \alpha_l H_l(K_c r) \cos l\theta. \tag{34}$$

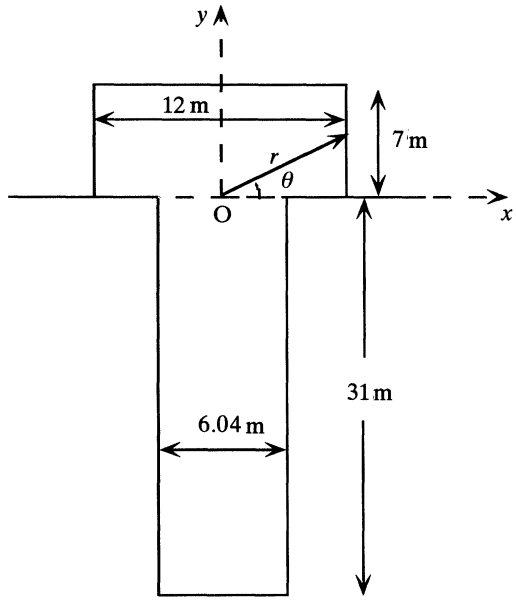

Figure 6. Rectangular harbour resonance problem. Waves incident from top.

Figure 7

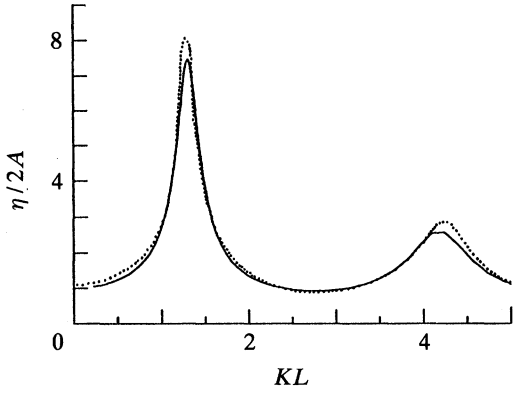

Figure 8

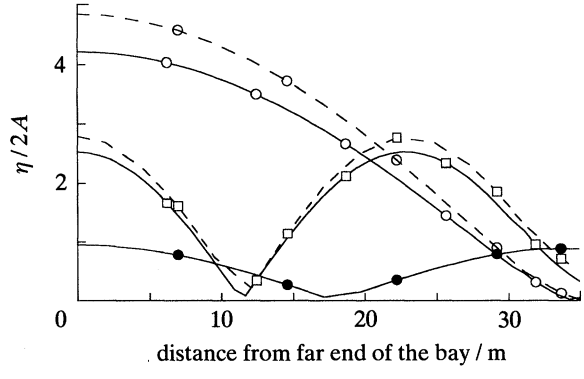

Figure 7. Wave height comparison for different wavelengths: ——, finite difference; - - - -, analytical.

Figure 8. Wave height comparison along central vertical axis of symmetry. (Dashed line finite-elements; solid line finite-differences. The curves are indistinguishable for $KL = 2.74$). ○, $KL = 1.48$; □, $KL = 4.27$; ●, $KL = 2.74$.

The procedure described in §§3 and 4 can now be implemented by simply replacing the original Φ^{I} by Φ^{IR} and (12) by (34).

Solutions are obtained using only about 800 grids of size $\Delta x = 0.604$ m and $\Delta y = 0.778$ m. For several wave periods, the resulting wave heights at the middle of the back wall are shown in figure 7. The analytical solution from Mei (1983) is also shown and the comparison is excellent. Further results along the central vertical axis of symmetry are shown in figure 8 for three cases. These include the results of another finite-element model; this model uses the conventional semicircular region to separate the computational region from the infinite superelement, and as noted in §1, can handle the radiation condition at infinity naturally with the variational

principle. The comparison in figure 8 is quite good. Some differences may be seen, however, these are attributed to the coarse resolution of the finite-element model. (The same grid as that shown in Chen & Houston (1987) was used.) Also the results near the resonant peaks are generally difficult to simulate perfectly (Dong & Al-Mashouk 1989), and minor differences in intermodel comparison are to be expected. The important point is that both models show essentially the same features and the new method of treating the radiation condition in finite-difference models creates no spurious reflections, even though the outer basin is extremely small.

6. Summary and conclusions

The treatment of open boundaries in wave models is generally considered a difficult problem. In the context of finite-difference elliptic models, the approach taken so far has been to approximate the boundary condition (which can cause spurious oscillations) or to enlarge the domain well beyond the region of interest (which increases the computational effort). While these methods may sometimes work satisfactorily, there is often no guarantee of their success ahead of time.

A method has therefore been devised to incorporate the radiation condition at infinity in a finite-difference model. (This has hitherto been possible only with finite-element models.) The method is based on using a Fourier–Bessel series to describe the scattered wave potential in the open ocean. However, matching this to the internal solutions along the contour Γ can be problematic. We therefore suggest an alternative criterion based on minimizing the overall error functional along Γ. An appropriate algorithm to incorporate this treatment of the open boundaries into the standard matrix equation is also described.

The procedure is verified using two standard test-cases that involved both long and short waves. Compared with previous works, satisfactory solutions are obtained with far fewer grids and/or with much smaller domains. No difficulty with spurious reflections was encountered and the results matched the analytical solutions very well. This 'exact' treatment of open boundaries can thus lead not only to improved solutions, but can also save computational effort. It can handle harbour and other coastal domains as well as open ocean problems.

Partial support for this work was received from the Maine Sea Grant College Program (National Oceanic & Atmospheric Administration), Grant NA16RG0157-01, and from the University of Maine Centre for Marine Studies. IBM3090 computing facilities were provided by the University of Maine.

Appendix

Here we obtain the derivatives of the vector $\{h\}$ and Φ^{I} along the outward normal direction on the open boundary. For illustration, we assume that the domain consists of four open boundaries (see figure 1). As mentioned in the text, the derivatives are computed on the dashed lines B′D′, D′C′, C′A′ and A′B′.

On B′D′, the out-normal derivatives of Φ^{I} is

$$\begin{aligned}\frac{\partial \Phi^{\mathrm{I}}}{\partial n} &= \frac{\partial \Phi^{\mathrm{I}}}{\partial r}\cos\theta - \frac{\partial \Phi^{\mathrm{I}}}{r\,\partial\theta}\sin\theta \\ &= \mathrm{i}A_0 K \exp\left[\mathrm{i}Kr\cos(\theta-\theta_0)\right]\left[\cos(\theta-\theta_0)\cos\theta+\sin(\theta-\theta_0)\sin\theta\right] \\ &= \mathrm{i}A_0 K\cos\theta_0 \exp\left[\mathrm{i}Kr\cos(\theta-\theta_0)\right]. \end{aligned} \tag{A 1}$$

Similarly, we can find derivatives of terms in vector $\{h\}$ on B′D′ as follows:

$$\frac{\partial(h)_j}{\partial n} \equiv \frac{\partial H_{j-1}(Kr)\cos(j-1)\theta}{\partial n}$$
$$= ((j-1)/r)H_{j-1}(Kr)\cos(j-2)\theta - KH_j(Kr)\cos(j-1)\theta\cos\theta, \quad \text{when } j \leqslant m+1, \tag{A 2}$$

$$\frac{\partial(h)_j}{\partial n} \equiv \frac{\partial H_i(Kr)\sin i\theta}{\partial n}$$
$$= (i/r)H_i(Kr)\sin(i-1)\theta - KH_{i+1}(Kr)\sin i\theta\cos\theta,$$
$$\text{when } j > m+1 \quad \text{and} \quad i = j-(m+1). \tag{A 3}$$

Similarly the following results are obtained for the derivatives on other three sides. On D′C′:

$$\frac{\partial \Phi^{\mathrm{I}}}{\partial n} = iA_0 K\sin\theta_0 \exp[iKr\cos(\theta-\theta_0)], \tag{A 4}$$

$$\frac{\partial(h)_j}{\partial n} \equiv \frac{\partial H_{j-1}(Kr)\cos(j-1)\theta}{\partial n}$$
$$= -((j-1)/r)H_{j-1}(Kr)\sin(j-2)\theta - KH_j(Kr)\cos(j-1)\theta\sin\theta,$$
$$\text{when } j \leqslant m+1, \tag{A 5}$$

$$\frac{\partial(h)_j}{\partial n} \equiv \frac{\partial H_i(Kr)\sin i\theta}{\partial n} = (i/r)H_i(Kr)\cos(i-1)\theta - KH_{i+1}(Kr)\sin i\theta\sin\theta,$$
$$\text{when } j > m+1 \quad \text{and} \quad i = j-(m+1). \tag{A 6}$$

On C′A′:

$$\partial \Phi^{\mathrm{I}}/\partial n = -\mathrm{i}A_0 K\cos\theta_0 \exp[\mathrm{i}Kr\cos(\theta-\theta_0)], \tag{A 7}$$

$$\frac{\partial(h)_j}{\partial n} \equiv \frac{\partial H_{j-1}(Kr)\cos(j-1)\theta}{\partial n}$$
$$= -((j-1)/r)H_{j-1}(Kr)\cos(j-2)\theta + KH_j(Kr)\cos(j-1)\theta\cos\theta, \quad \text{when } j \leqslant m+1, \tag{A 8}$$

$$\frac{\partial(h)_j}{\partial n} \equiv \frac{\partial H_i(Kr)\sin i\theta}{\partial n}$$
$$= -(i/r)H_i(Kr)\sin(i-1)\theta + KH_{i+1}(Kr)\sin i\theta\cos\theta,$$
$$\text{when } j > m+1 \quad \text{and} \quad i = j-(m+1). \tag{A 9}$$

On A′B′:

$$\partial \Phi^{\mathrm{I}}/\partial n = -\mathrm{i}A_0 K\sin\theta_0 \exp[\mathrm{i}Kr\cos(\theta-\theta_0)], \tag{A 10}$$

$$\frac{\partial(h)_j}{\partial n} \equiv \frac{\partial H_{j-1}(Kr)\cos(j-1)\theta}{\partial n}$$
$$= \frac{j-1}{r}H_{j-1}(Kr)\sin(j-2)\theta + KH_j(Kr)\cos(j-1)\theta\sin\theta, \quad \text{when } j \leqslant m+1, \tag{A 11}$$

$$\frac{\partial(h)_j}{\partial n} \equiv \frac{\partial H_i(Kr)\sin i\theta}{\partial n}$$
$$= -(i/r)H_i(Kr)\cos(i-1)\theta + KH_{i+1}(Kr)\sin i\theta\sin\theta,$$
$$\text{when } j > m+1 \quad \text{and} \quad i = j-(m+1). \tag{A 12}$$

References

Berkhoff, J. C. W. 1976 *Mathematical models for simple harmonic linear water waves.* Wave Refraction and Diffraction, Publ. 163, Delft Hydraulics Laboratory.

Berkhoff, J. C. W., Booij, N. & Radder, A. C. 1982 Verification of numerical wave propagation models for simple harmonic linear water waves. *Coastal Engng* **6**, 255–279.

Chen, H. S. & Houston, J. R. 1987 Calculation of water level oscillation in coastal harbors. Instructional Rep. CERC-87-2, Coastal Engng Research Center, WES, Vicksburg.

Dalrymple, R. A. & Martin, P. A. 1992 Perfect boundary conditions for parabolic water-wave models. *Proc. R. Soc. Lond.* A **437**, 41–54.

Dong, P. & Al-Mashouk, M. 1989 Comparison of transient and steady state wave models for harbor resonance. In *Hydraulic and environmental modeling of coastal, estuarine and river waters* (ed. R. A. Falconer *et al.*). University of Bradford, U.K.

Homma, S. 1950 On the behaviour of seismic sea waves around circular island. *Geophys. Mag.* **21**, 199.

Houston, J. R. 1981 Combined refraction and diffraction of short waves using the finite element method. *Appl. Ocean Res.* **3**, 163–170.

Jonsson, I. G., Skovgaard, O. & Brink-Kjaer, O. 1976 Diffraction and refraction calculations for waves incident on an island. *J. mar. Res.* **343**, 468–496.

Kirby, J. T. 1989 A note on parabolic radiation boundary conditions for elliptic wave calculations. *Coastal Engng* **13**, 211–218.

Kostense, J. K., Meijer, K. L., Dingemans, M. W., Mynett, A. E. & van den Bosch, P. 1986 Wave energy dissipation in arbitrarily shaped harbours of variable depth. In *Proc. 20th Int. Conf. Coastal Engng*, pp. 2002–2016.

Li, B. & Anastasiou, K. 1992 Efficient elliptic solvers for the mild-slope equation using the multigrid method. *Coastal Engng* **16**, 245–266.

Lillycrop, L. S., Bratos, S. M. & Thompson, E. F. 1990 Wave-response of proposed improvements to the shallow draft harbor at Kawaihae, Hawaii. CERC-90-8. Coastal Engng Research Center, WES, Vicksburg.

Mei, C. C. 1983 *The applied dynamics of ocean surface waves.* New York: Wiley.

Madsen, P. A. & Larsen, J. 1987 An efficient finite-difference approach to the mild-slope equation. *Coastal Engng* **11**, 329–351.

Panchang, V. G., Cushman-Roisin, B. & Pearce, B. R. 1988 Combined refraction-diffraction of short waves for large domains. *Coastal Engng* **12**, 133–156.

Panchang, V. G., Pearce, B. R., Ge, W. & Cushman-Roisin, B. 1991 Solution to the mild-slope wave problem by iteration. *Appl. Ocean Res.* **13**, 187–199.

Radder, A. C. 1979 On the parabolic equation method for water-wave propagation. *J. Fluid Mech.* **95**, 159–176.

Smith, R. & Sprinks, T. 1975 Scattering of surface waves by a conical island. *J. Fluid Mech.* **72**, 373–384.

Tsay, T.-K. & Liu, P. L.-F. 1983 A finite element model for wave refraction and diffraction. *Appl. Ocean Res.* **5**, 30–37.

Received 25 September 1992; accepted 25 November 1992